

# Nonmonotonic size dependence of the critical concentration in 2D percolation of straight rigid rods under equilibrium conditions

D. A. Matoz-Fernandez, D. H. Linares and A. J. Ramirez-Pastor\*

Departamento de Física, Instituto de Física Aplicada,  
Universidad Nacional de San Luis-CONICET,  
Chacabuco 917, D5700BWS San Luis, Argentina

February 9, 2018

## Abstract

Numerical simulations and finite-size scaling analysis have been carried out to study the percolation behavior of straight rigid rods of length  $k$  ( $k$ -mers) on two-dimensional square lattices. The  $k$ -mers, containing  $k$  identical units (each one occupying a lattice site), were adsorbed at equilibrium on the lattice. The process was monitored by following the probability  $R_{L,k}(\theta)$  that a lattice composed of  $L \times L$  sites percolates at a concentration  $\theta$  of sites occupied by particles of size  $k$ . A nonmonotonic size dependence was observed for the percolation threshold, which decreases for small particles sizes, goes through a minimum, and finally asymptotically converges towards a definite value for large segments. This striking behavior has been interpreted as a consequence of the isotropic-nematic phase transition occurring in the system for large values of  $k$ . Finally, the universality class of the model was found to be the same as for the random percolation model.

**Keywords:** *Percolation, Multisite-Occupancy, Isotropic-nematic phase transition, Monte Carlo Simulation*

---

\***Corresponding author:** Dr. A. J. Ramirez-Pastor, Departamento de Física, Instituto de Física Aplicada, Universidad Nacional de San Luis-CONICET, Chacabuco 917, D5700BWS San Luis, Argentina  
**Email:** antorami@unsl.edu.ar

# 1 Introduction

The percolation problem is a topic being increasingly considered in statistical physics. One reason for this current interest is that it is becoming clear that generalizations of the pure percolation problem are likely to have extensive applications in science and technology [1, 2, 3, 4, 5]. Although it is a purely geometric phenomenon, the phase transition involved in the process can be described in terms of an usual second-order phase transition. This mapping to critical phenomena made percolation a full part of the theoretical framework of collective phenomena and statistical physics.

Despite of the number of contributions to this problem, there are many aspects which are not yet completely solved. In fact, most of the studies are devoted to the percolation of objects whose size coincides with the size of the lattice site (single occupancy). However, if some sort of correlation exists, like particles occupying several  $k$  contiguous lattice sites ( $k$ -mers), the statistical problem becomes exceedingly difficult and a few studies have been devoted to understanding the percolation of elements occupying more than one site (bond) [6, 7, 8, 9, 10, 11, 12, 13, 14, 15, 16, 17].

In two previous articles [13, 17], referred to as papers I and II, respectively, the percolation of straight rigid rods on 2D lattices was studied. In paper I, linear  $k$ -mers were deposited randomly and irreversibly. It was established that (1) the percolation threshold exhibits an exponentially decreasing function when it is plotted as a function of the  $k$ -mer size and (2) the problem belongs to the same universality class that the random percolation regardless the value of  $k$  used. Paper II was devoted to the study of aligned rigid rods on square lattices. In this case, the  $k$ -mers were irreversibly deposited along one of the directions of the lattice. The results obtained revealed that (i) the percolation threshold monotonically decreases with increasing  $k$ ; (ii) for any value of  $k$  ( $k > 1$ ), the percolation threshold is higher for aligned rods than for isotropically deposited rods; (iii) the phase transition occurring in the system belongs to the standard random percolation universality class; and (iv) the intersection point of the percolation cumulant curves for different system sizes exhibits a nonuniversal critical behavior, varying continuously with changing the  $k$ -mer size.

On the other hand, numerous experimental and numerical studies have been recently devoted to the analysis of equilibrium properties in systems of non-spherical particles [18, 19, 20, 21, 22, 23, 24, 25, 26]. Of special interest are those studies dealing with lattice versions of the present problem, where the situation is much less clear than in the continuum case. In this line, a system of straight rigid rods of length  $k$  on a square lattice, with two allowed orientations, was recently studied by Monte Carlo simulations [22]. The authors found strong numerical evidence on the existence of an isotropic-nematic (IN)

phase transition at intermediate densities for  $k \geq 7$ . The nematic phase, characterized by a big domain of parallel  $k$ -mers, is separated from the isotropic phase by a continuous transition occurring at a finite density. The accurate determination of the critical exponents, along with the behavior of Binder cumulants, showed that the transition from the low-density disordered phase to the intermediate-density ordered phase belongs to the 2D Ising universality class for square lattices and the three-state Potts universality class for honeycomb and triangular lattices [23, 24]. In addition, the comparison between the configurational entropy of the system and that corresponding to a fully aligned system [25, 26] (i) confirmed the existence of a IN phase transition at intermediate densities for long rods, (ii) allowed us to estimate the minimum value of  $k$ , which leads to the formation of a nematic phase, and (iii) provided an interesting interpretation of this critical value.

Later, the dependence of the critical density on the magnitude of the lateral interactions was studied for a system of attractive rigid rods on square lattices with two allowed orientations [27, 28]. The obtained results revealed that the orientational order survives in a wide range of lateral interactions.

A notable feature is that nematic order is only stable for sufficiently large aspect ratios while systems of short rods do not show nematic order at all. The long-range orientational order also disappears in the case of irreversible adsorption (as is the case of papers I and II), where the distribution of adsorbed objects is different from that obtained at equilibrium. Thus, the irreversible adsorption leads to intermediate states characterized by an isotropic distribution of the directions of the adsorbed molecules, and to a final state (known as jamming state), in which no more objects can be deposited due to the absence of free space of appropriate size and shape (the jamming state has infinite memory of the process and the orientational order is purely local) [29].

It is of interest then to study the percolation problem of  $k$ -mers at equilibrium, not only because of this problem has not been treated in the literature, but also because, depending on the values of the density and the size  $k$ , the model leads either to an isotropic system (as studied in paper I) or an anisotropic system (as studied in paper II). In this sense, the aim of the present work is to study, by Monte Carlo (MC) simulations and finite-size scaling analysis, the effect of the orientational order on the percolation properties for a system of rigid rods adsorbed at equilibrium on two-dimensional square lattices.

## 2 Model and Monte Carlo simulation

The calculations have been developed for straight rigid rods of length  $k$ , with  $k$  ranging between 2 and 12. Small adsorbates with spherical symmetry would correspond to the

monomer limit ( $k = 1$ ). The distance between  $k$ -mer units is assumed to be equal to the lattice constant; hence exactly  $k$  sites are occupied by a  $k$ -mer when adsorbed. The surface was represented as a 2D square lattice of  $M = L \times L$  adsorptive sites with periodic boundary conditions. The only interaction between different rods is hard-core exclusion: no site can be occupied by more than one  $k$ -mer.

To describe a system of  $N$   $k$ -mers adsorbed on  $M$  sites at a given temperature  $T$  and chemical potential  $\mu$ , the occupation variable  $c_j$  was introduced ( $c_j = 0$  or  $1$ , if the site  $j$  is empty or occupied by a  $k$ -mer unit, respectively). Then the adsorbed phase is characterized by the Hamiltonian  $H = (\epsilon_0 - \mu) \sum_j c_j$ , where the sum run over the  $M$  sites and  $\epsilon_0$  is the adsorption energy of a  $k$ -mer unit (in the simulations,  $\epsilon_0$  is set equal to zero without any loss of generality).

The thermodynamic equilibrium is reached in the grand canonical ensemble by using the hyper-parallel tempering Monte Carlo (HPTMC) simulation method [30, 31] combined with an efficient cluster algorithm (the pocket algorithm) [32].

The HPTMC method consists in generating a compound system of  $R$  noninteracting replicas of the system under study. The  $i$ -th replica is associated with a chemical potential  $\mu_i$ . To determine the set of chemical potentials,  $\{\mu_i\}$ , we set the lowest chemical potential,  $\mu_1$ , in the isotropic phase where relaxation (correlation) time is expected to be very short and there exists only one minimum in the free energy space. On the other hand, the highest chemical potential,  $\mu_R$ , is set in the nematic phase whose properties we are interested in. Finally, the difference between two consecutive chemical potentials,  $\mu_i$  and  $\mu_{i+1}$  with  $\mu_i < \mu_{i+1}$ , is set as  $\Delta\mu = (\mu_1 - \mu_R)/(R - 1)$  (equally spaced chemical potentials). The parameters used in the present study were as follows:  $R = 40$ ,  $\mu_1 = -2.5$  and  $\mu_R = 2.375$ . With these values of the chemical potential, the corresponding values of the surface coverage varied from  $\theta_1(\mu_1) \approx 0.21$  to  $\theta_R(\mu_R) \approx 0.88$  for  $k = 2$ , and from  $\theta_1(\mu_1) \approx 0.33$  to  $\theta_R(\mu_R) \approx 0.81$  for  $k = 12$ .

Under these conditions, the algorithm to carry out the simulation process is built on the basis of two major subroutines: *replica-update* and *replica-exchange*.

*Replica-update*: The adsorption-desorption and pocket procedure is as follows: (1) One out of  $R$  replicas is randomly selected. (2) A linear  $k$ -uple of nearest-neighbor sites, belonging to the replica selected in (1), is chosen at random. Then, if the  $k$  sites are empty, an attempt is made to deposit a rod with probability  $W = \min\{1, \exp(\beta\mu)\}$ ; if the  $k$  sites are occupied by units belonging to the same  $k$ -mer, an attempt is made to desorb this  $k$ -mer with probability  $W = \min\{1, \exp(-\beta\mu)\}$ ; and otherwise, the attempt is rejected. In addition, the pocket algorithm [32] is applied in order to reach equilibrium in a reasonable time. This algorithm includes the following steps: (1) Choose randomly a lattice symmetry axis and a seed  $k$ -mer. The seed  $k$ -mer now is the sole element of a

set  $\mathcal{P}$  and the rest of  $k$ -mers belongs to a set  $\mathcal{O}$ . (2) Move elements from the set  $\mathcal{P}$  to  $\mathcal{O}$  in the following way: Pick up an arbitrary element  $i$  of  $\mathcal{P}$  and reflect with respect to the symmetry axis. If  $i$  overlaps with other elements of  $\mathcal{O}$ , the latter are transferred from  $\mathcal{O}$  to  $\mathcal{P}$ . (3) Repeat the step (2) until the set  $\mathcal{P} = \emptyset$ .

*Replica-exchange*: Exchange of two configurations  $X_i$  and  $X_j$ , corresponding to the  $i$ -th and  $j$ -th replicas, respectively, is tried and accepted with probability  $W = \min\{1, \exp(-\Delta)\}$ . Where  $\Delta$  in a nonthermal grand canonical ensemble is given by  $[-\beta(\mu_j - \mu_i)(N_j - N_i)]$ , and  $N_i$  ( $N_j$ ) represents the number of particles of the  $i$ -th ( $j$ -th) replica.

The complete simulation procedure is the following: (1) replica-update, (2) replica-exchange, and (3) repeat from step (1)  $RM$  times. This is the elementary step in the simulation process or Monte Carlo step (MCs).

For each value of the chemical potential  $\mu_i$ , the equilibrium state can be well reproduced after discarding the first  $r_0$  MCs. Then, a set of  $m$  samples in thermal equilibrium is generated. The corresponding surface coverage  $\theta_i(\mu_i)$  is obtained through simple averages over the  $m$  samples ( $m$  MCs).

As mentioned before in Ref. [22], the relaxation time increases very quickly as the  $k$ -mer size increases. Consequently, MC simulations for large adsorbates are very time consuming and may produce artifacts related to non-accurate equilibrium states. In order to discard this possibility, equilibration times  $r_0$  of the order  $O(10^6)$  MCs were used in this study, with an effort reaching almost the limits of our computational capabilities [33].

### 3 Finite-size scaling results

The central idea of the pure percolation theory is based in finding the minimum concentration of elements (sites or bonds) for which a cluster extends from one side to the opposite one of the system. At this particular value of the concentration, the percolation threshold  $\theta_c$ , a second-order phase transition occurs in the system, which is characterized by well-defined critical exponents [2].

The finite-size scaling theory [34] gives us the basis to achieve the percolation threshold and the critical exponents of a system with a reasonable accuracy. For this purpose, the probability  $R = R_{L,k}^X(\theta)$  that a  $L \times L$  lattice percolates at a concentration  $p$  of sites occupied by rods of size  $k$  can be defined [2, 35]. Here, the following definitions can be given according to the meaning of  $X$ : a)  $R_{L,k}^{R(D)}(\theta)$  = the probability of finding a rightward (downward) percolating cluster; and b)  $R_{L,k}^U(\theta)$  = the probability of finding either a rightward **or** a downward percolating cluster.

In the Monte Carlo (MC) simulations, each run consists of the following steps: (a)

the construction of  $m = 2 \times 10^5$  samples for the desired fraction  $\theta(\mu)$  of occupied sites (according to the HPTMC method described above); and (b) the cluster analysis by using the Hoshen and Kopelman algorithm [36]. In the last step, the existence of a percolating island is verified for each sample. The spanning cluster could be determined by using the criteria  $R$ ,  $D$  and  $U$ . This scheme is carried out for obtaining the number  $m^X$  of samples for which a percolating cluster of the desired criterion  $X$  is found. Then,  $R_{L,k}^X(\theta) = m^X/m$  is defined and the procedure is repeated for different values of  $\theta$ ,  $L$  and  $k$ .

Besides the parameter  $R$ , the percolation order parameter  $P = \langle S_L \rangle / L^2$  [37, 38] has been measured, where  $S_L$  represents the size of the largest cluster and  $\langle \dots \rangle$  means the average over the  $m$  samples. The corresponding percolation susceptibility  $\chi$  has also been calculated,  $\chi = [\langle S_L^2 \rangle - \langle S_L \rangle^2] / L^2$ .

In Figure 1, the probability  $R_{L,k}^U(\theta)$  is presented for  $k = 3$  (left),  $k = 5$  (middle) and  $k = 7$  (right) and different lattice sizes  $L/k = 5, 10, 15, 20$  [39], as indicated in the caption of the figure. Several conclusions can be drawn from the figure. First, curves cross each other in a unique point  $R_k^{X*}$  (measured in the vertical axes), which depends on the criterion  $X$  used (data corresponding to criteria  $R$  and  $D$  are not shown in the figure for clarity) and those points are located at very well defined values in the  $\theta$ -axes determining the critical percolation threshold (measured in the horizontal axes) for each  $k$ . The values of  $\theta_c(k)$  obtained by following the procedure of Figure 1 are collected in Table 1 and are plotted in Figure 2a (full circles). A nonmonotonic size dependence is observed for the percolation threshold, which decreases for small particles sizes, goes through a minimum around  $k = 5$ , and finally asymptotically converges towards a definite value for large segments. This striking behavior can be interpreted as a consequence of the IN phase transition occurring in the system for large values of  $k$  [22, 23, 24, 25, 26]. To understand this effect, it is convenient first to recall some results about percolation of straight rigid rods isotropically deposited (or isotropic  $k$ -mers) [13] and straight rigid rods deposited along one of the directions of the lattice (or aligned  $k$ -mers) [17].

In the first case (isotropic  $k$ -mers) [13], the rods are deposited randomly and irreversibly. The process is as follows: a linear  $k$ -uple of nearest-neighbor sites is randomly selected; if it is vacant, a  $k$ -mer is then deposited on those sites. Otherwise, the attempt is rejected. This filling process, known as Random Sequential Adsorption model, leads to states characterized by an isotropic distribution of the directions of the adsorbed  $k$ -mers. In the case of aligned  $k$ -mers [17], the adsorption process is also irreversible, but this time the  $k$ -mers are deposited along one of the directions of the lattice, forming a nematic phase.

As it can be observed from Figure 2a, the percolation threshold curves corresponding to isotropic (open circles) and aligned (open squares)  $k$ -mers decrease upon increasing  $k$ .

At the beginning, for small values of  $k$ , the curves rapidly decrease. However, they flatten out for larger values of  $k$  and finally asymptotically converge towards a definite value  $\theta_c^*$  (as  $k \rightarrow \infty$ ), being  $\theta_c^* \approx 0.46$  for isotropic  $k$ -mers and  $\theta_c^* \approx 0.54$  for aligned  $k$ -mers.

Now, the nonmonotonic behavior observed in Figure 2a can be explained on the basis of the results for isotropic and aligned  $k$ -mers. In fact, for small values of  $k$ , there is no orientational order in the equilibrium adlayer and  $\theta_c(k)$  decreases following the curve corresponding to isotropic  $k$ -mers. On the other hand, for large values of  $k$ , a nematic phase, characterized by a big domain of parallel  $k$ -mers, is formed on the surface at an intermediate density  $\theta_{IN}$  [22, 23, 24, 25, 26]. The values of  $\theta_{IN}$  reported in Ref. [25] are listed in the third column of Table 1. For  $k \geq 9$ ,  $\theta_c > \theta_{IN}$  and, consequently, (1) the percolation properties of the orientational phase are similar to the ones corresponding to perfectly aligned  $k$ -mers and (2)  $\theta_c(k)$  follows the curve corresponding to aligned  $k$ -mers. As a consequence of the behavior of  $\theta_c(k)$  in the limits of small and large  $k$ -mers, a marked minimum is observed at intermediate values of  $k$ .

Typical equilibrium states are shown schematically in parts (b)-(d) of Figure 2. In the case of Figure 2b [point  $i$  in Figure 2a:  $k = 2$  and  $\theta \approx 0.53$ ], the equilibrium state corresponds to an isotropic and nonpercolating state. The situation is different in Figure 2c [point  $f$  in Figure 2a:  $k = 5$  and  $\theta \approx 0.53$ ], where the equilibrium state is an isotropic and percolating state. Thin bars represent isolated  $k$ -mers and thick bars (red bars in the online version) correspond to  $k$ -mers belonging to the percolating cluster. Finally, a nematic and nonpercolating state is observed in Figure 2d [point  $j$  in Figure 2a:  $k = 10$  and  $\theta \approx 0.53$ ].

A second conclusion of Figure 1 is that the crossing points of the percolation cumulants  $R_k^{U*}$  (as  $R_k^{R*}$  and  $R_k^{D*}$ ) vary as the  $k$ -mer size is increased. This behavior was already observed in the case of perfectly aligned  $k$ -mers irreversibly deposited on 2D lattices [17] and can be attributed to the strong anisotropy introduced in the system by the IN phase transition occurring for large  $k$ -mers. In the case of thermal transitions, the link between anisotropy and a nonuniversal behavior of the intersection point of the cumulants has been discussed in [45, 46]. In fact, as pointed out by Selke et al. [45, 46], the measure of the cumulant intersection may depend on various details of the model, which do not affect the universality class, in particular, the boundary condition, the shape of the lattice, and the anisotropy of the system. In order to confirm or discard this hypothesis, the critical exponents  $\nu$ ,  $\beta$  and  $\gamma$  were calculated as follows.

The value of  $\nu$  can be obtained through the scaling relationship for  $R_{L,k}^X(\theta)$

$$R_{L,k}^X(\theta) = \overline{R_k^X} [(\theta - \theta_c) L^{1/\nu}], \quad (1)$$

being  $\overline{R_k^X}(u)$  the scaling function and  $u \equiv (\theta - \theta_c) L^{1/\nu}$ . Then, the maximum of the

derivative of Eq. (1) leads to  $(dR_{L,k}^X/d\theta)_{\max} \propto L^{1/\nu}$ .

In the inset of Figure 3,  $(dR_{L,k}^X/d\theta)_{\max}$  has been plotted as a function of  $L/k$  (note the log-log scale) for different  $k$ -mers as indicated. According to Eq. (1) the slope of each line corresponds to  $1/\nu$ . As it can be observed, the slopes of the curves remain constant (and close to  $3/4$ ) for all values of  $k$ . The results coincide, within numerical errors, with the exact value of the critical exponent of the ordinary percolation  $\nu = 4/3$ .

The scaling behavior can be further tested by plotting  $R_{L,k}^X(\theta)$  vs  $(\theta - \theta_c) L^{1/\nu}$  and looking for data collapsing. Using the values of  $\theta_c$  previously calculated and the exact value  $\nu = 4/3$ , an excellent scaling collapse was obtained (Figure 3) for all value of  $k$ -mer size. This leads to independent control and consistency check of the numerical value of the critical exponent  $\nu$ .

The critical exponents  $\beta$  and  $\gamma$  were obtained from the scaling behavior of  $P$  and  $\chi$  [2],

$$P = L^{-\beta/\nu} \overline{P} [|\theta - \theta_c| L^{1/\nu}] , \quad (2)$$

and

$$\chi = L^{\gamma/\nu} \overline{\chi} [(\theta - \theta_c) L^{1/\nu}] , \quad (3)$$

where  $\overline{P}$  and  $\overline{\chi}$  are scaling functions for the respective quantities. According to Eqs. (2) and (3), Figure 4 shows the collapse of the curves of  $P$  and  $\chi$  (inset) for a typical  $k$ -mer size ( $k = 5$ ) and different lattice sizes as indicated. The study was repeated for all studied values of  $k$  (these data are not shown here for lack of space). The data scaled extremely well using the exact percolation exponents  $\beta = 5/36$  and  $\gamma = 43/18$ . The results obtained in Figures 3 and 4 clearly supports that, as in the case of isotropic rods [13], the universality class of the problem does not depend on the  $k$ -mer size.

## 4 Conclusions

In this work, Monte Carlo simulations and finite-size scaling theory have been used to study the percolation properties of straight rigid rods of length  $k$  adsorbed at equilibrium on two-dimensional square lattices.

A nonmonotonic size dependence was found for the percolation threshold  $\theta_c$ , which decreases for small particles sizes [following the curve of  $\theta_c(k)$  for  $k$ -mers irreversibly and isotropically deposited], goes through a minimum, and finally asymptotically converges towards a definite value for large segments [following the curve of  $\theta_c(k)$  for aligned  $k$ -mers irreversibly deposited along one of the directions of the lattice]. This striking behavior has been interpreted as a consequence of the IN phase transition occurring in the system for large values of  $k$ . Finally, the analysis of the critical exponents  $\nu$ ,  $\beta$  and  $\gamma$  revealed



that the percolation phase transition involved in the problem considered in the present paper belongs to the same universality class of the ordinary random percolation.

## **Acknowledgment**

This work was supported in part by CONICET (Argentina) under project number PIP 112-200801-01332; Universidad Nacional de San Luis (Argentina) under project 322000 and the National Agency of Scientific and Technological Promotion (Argentina) under project PICT-2010-1466.

## References

- [1] R. Zallen, *The Physics of Amorphous Solids* (Wiley & Sons, New York, 1983).
- [2] D. Stauffer, A. Aharony, *Introduction to Percolation Theory*, 2nd ed. (Taylor & Francis, London, 1994).
- [3] M. Sahimi, *Applications of Percolation Theory* (Taylor & Francis, London, 1994); *Flow and Transport in Porous Media and Fractured Rock* (VCH, Weinheim, Germany, 1995).
- [4] G. Grimmett, *Percolation* (Springer-Verlag, Berlin, 1999).
- [5] B. Bollobás, O. Riordan, *Percolation* (Cambridge University Press, New York, 2006).
- [6] H. Harder, A. Bunde, W. Dieterich, J. Chem. Phys. **85**, 4123 (1986).
- [7] Z. Gao, Z. R. Yang, Physica A **255**, 242 (1998).
- [8] H. Holloway, Phys. Rev. B **37**, 874 (1988).
- [9] M. Dolz, F. Nieto, A. J. Ramirez-Pastor, Eur. Phys. J. B **43**, 363 (2005); Phys. Rev. E **72**, 066129 (2005); Physica A **374**, 239 (2007).
- [10] Y. Leroyer, E. Pommiers, Phys. Rev. B **50**, 2795 (1994).
- [11] B. Bonnier, M. Hontebeyrie, Y. Leroyer, C. Meyers, E. Pommiers, Phys. Rev. E **49**, 305 (1994).
- [12] V. Cornette, A. J. Ramirez-Pastor, F. Nieto, Physica A **327**, 71 (2003).
- [13] V. Cornette, A. J. Ramirez-Pastor, F. Nieto, Eur. Phys. J. B **36**, 391 (2003).
- [14] V. Cornette, F. Nieto, A. J. Ramirez-Pastor, Phys. Lett. A **353**, 452 (2006).
- [15] V. Cornette, A. J. Ramirez-Pastor, F. Nieto, J. Chem. Phys. **125**, 204702 (2006).
- [16] V. A. Cherkasova, Y. Y. Tarasevich, N. I. Lebovka, N. V. Vygornitskii, Eur. Phys. J. B **74**, 205 (2010).
- [17] P. Longone, P. M. Centres, A.J. Ramirez-Pastor, Phys. Rev. E **85**, 011108 (2012).
- [18] J. Viamontes, P. W. Oakes, J. X. Tang, Phys. Rev. Lett. **97**, 118103 (2006).
- [19] C. De Michele, R. Schilling, F. Sciortino, Phys. Rev. Lett. **98**, 265702 (2007).

- [20] R. L. C. Vink, Phys. Rev. Lett. **98**, 217801 (2007).
- [21] A. Cuetos, M. Dijkstra, Phys. Rev. Lett. **98**, 095701 (2007).
- [22] A. Ghosh, D. Dhar, Eur. Phys. Lett. **78**, 20003 (2007).
- [23] D. A. Matoz-Fernandez, D. H. Linares, A. J. Ramirez-Pastor, Europhys. Lett. **82**, 50007 (2008).
- [24] D. A. Matoz-Fernandez, D. H. Linares, A. J. Ramirez-Pastor, Physica A **387**, 6513 (2008).
- [25] D. A. Matoz-Fernandez, D. H. Linares, A. J. Ramirez-Pastor, J. Chem. Phys. **128**, 214902 (2008).
- [26] D. H. Linares, F. Romá, A. J. Ramirez-Pastor, J. Stat. Mech. **2008**, P03013.
- [27] P. Longone, D. H. Linares, A. J. Ramirez-Pastor, Papers in Physics **1**, 010005 (2009).
- [28] P. Longone, D. H. Linares, A. J. Ramirez-Pastor, J. Chem. Phys. **132**, 184701 (2010).
- [29] J. W. Evans, Rev. Mod. Phys. **65**, 1281 1993.
- [30] Q. Yan, J. J. de Pablo, J. Chem. Phys. **113**, 1276 (2000).
- [31] K. Hukushima, K. Nemoto, J. Phys. Soc. Jpn. **65**, 1604 (1996).
- [32] W. Krauth, R. Moessner, Phys. Rev. B **67**, 064503 (2003).
- [33] As an example, it took about 90 days to obtain the adsorption isotherm corresponding to  $k = 12$  and  $L/k = 20$  on one node of the BACO parallel cluster. This facility, located at Instituto de Física Aplicada, Universidad Nacional de San Luis-CONICET, San Luis, Argentina, consists of 50 CPUs each with an Intel Core i7 processor running at 2.93 GHz and 512MB of RAM per core.
- [34] K. Binder, Rep. Prog. Phys. **60**, 488 (1997).
- [35] F. Yonezawa, S. Sakamoto, M. Hori, Phys. Rev. B **40**, 636 (1989); Phys. Rev. B **40**, 650 (1989).
- [36] J. Hoshen, R. Kopelman, Phys. Rev. B **14**, 3438 (1976); J. Hoshen, R. Kopelman, E. M. Monberg, J. Stat. Phys. **19**, 219 (1978).
- [37] S. Biswas, A. Kundu, A. K. Chandra, Phys. Rev. E **83**, 021109 (2011).

- [38] A. K. Chandra, Phys. Rev. E **85**, 021149 (2012)
- [39] As in previous work [13], the ratio  $L/k$  is kept constant for avoiding spurious effects due to the  $k$ -mer size in comparison with the lattice size.
- [40] M. E. J. Newman, R. M. Ziff, Phys. Rev. Lett. **85**, 4104 (2000).
- [41] P. M. C. de Oliveira, R. A. Nóbrega, D. Stauffer, Braz. J. Phys. **33**, 616 (2003).
- [42] M. J. Lee, Phys. Rev. E **76**, 027702 (2007).
- [43] X. Feng, Y. Deng, H. W. J. Blöte, Phys. Rev. E **78**, 031136 (2008).
- [44] M. J. Lee, Phys. Rev. E **78**, 031131 (2008).
- [45] W. Selke, L. N. Shchur, J. Phys. A **38**, L739 (2005).
- [46] W. Selke, J. Stat. Mech.: Theory Exp. **2007**, P04008.

# Table and Figure Captions

Table 1: Values of the percolation threshold  $\theta_c$  for  $k$  ranging from 1 to 12 and of the isotropic-nematic critical density  $\theta_{IN}$  [25] for  $k$  between 7 to 12. Note that the IN phase transition on a square lattice with two allowed orientations occurs only for  $k \geq 7$  [22, 23, 24, 25, 26]. In the case of  $k = 1$ , the problem of percolation of monomers on square lattices has been one of the most studied percolation models in the literature, and the percolation threshold has been measured multiple times as  $0.592746xx$ , where the last two decimal places (and error) are 21(13) [40], 21(33) [41], 03(09) [42], and 06(05) [43]. For a complete overview on this topic we refer the reader to Ref. [44].

Fig. 1: Fraction of percolating lattices  $R_{L,k}^U$  as a function of the concentration  $\theta$  for  $k = 3$  (left),  $k = 5$  (middle) and  $k = 7$  (right) and different lattice sizes:  $L/k = 5$ , diamonds;  $L/k = 10$ , squares;  $L/k = 15$ , circles and  $L/k = 20$ , triangles. Horizontal dashed lines show the intersection points  $R_k^{X*}$ . Vertical dashed line denotes the percolation threshold  $\theta_c$  in the thermodynamic limit.

Fig. 2: (Color online) (a) The percolation threshold  $\theta_c$  as a function of  $k$  for straight rigid rods on 2D square lattices and three different adsorption processes: nematic irreversible adsorption (open squares), isotropic irreversible adsorption (open circles) and equilibrium adsorption (solid circles). The dashed lines are simply a guide for the eye. In all cases, the error bar is smaller than the size of the symbols. The asymptotic limits,  $\theta_c^*$ ,  $[\theta_c(k)$  for  $k \rightarrow \infty]$  are shown. (b) Schematic representation of the equilibrium state for  $k = 2$  and  $\theta \approx 0.53$  (point  $i$  in the figure). (c) Same as (b) for  $k = 5$  and  $\theta \approx 0.53$  (point  $f$  in the figure). Thin bars represent isolated  $k$ -mers and thick bars (red bars in the online version) correspond to  $k$ -mers belonging to the percolating cluster. (d) Same as (b) for  $k = 10$  and  $\theta \approx 0.53$  (point  $j$  in the figure).

Fig. 3: Data collapsing of the fraction of percolating samples  $R_{L,k}^U(\theta)$  as a function of the argument  $(\theta - \theta_c) L^{1/\nu}$ . Each set of curves corresponds to a different value of  $k$  as indicated. For each  $k$ , different lattice sizes ( $L/k = 5, 10, 15$  and  $20$ ) have been considered. Inset:  $\ln\left(\frac{dR_{L,k}^U}{d\theta}\right)_{\max}$  as a function of  $\ln(L/k)$  for different values of  $k$  as indicated. According to Eq. (1) the slope of each line corresponds to  $1/\nu$ .

Fig. 4: Data collapsing of the order parameter,  $PL^{\beta/\nu}$  vs  $|\theta - \theta_c|L^{1/\nu}$ , and of the susceptibility,  $\chi L^{-\gamma/\nu}$  vs  $(\theta - \theta_c) L^{1/\nu}$  (inset) for  $k = 5$ . The plots were made using the exact percolation exponents  $\nu = 4/3$ ,  $\beta = 5/36$  and  $\gamma = 43/18$ .

Table 1

$k$ – mer size, $k$	percolation threshold, $\theta_c$	isotropic – nematic critical density, $\theta_{IN}$
1	0.592746 $xx(yy)$	– – –
2	0.586(1)	– – –
3	0.575(1)	– – –
4	0.567(1)	– – –
5	0.563(1)	– – –
6	0.559(1)	– – –
7	0.593(1)	0.729(3)
8	0.586(1)	0.648(3)
9	0.575(1)	0.569(3)
10	0.567(1)	0.502(3)
11	0.563(1)	0.457(5)
12	0.559(1)	0.413(5)

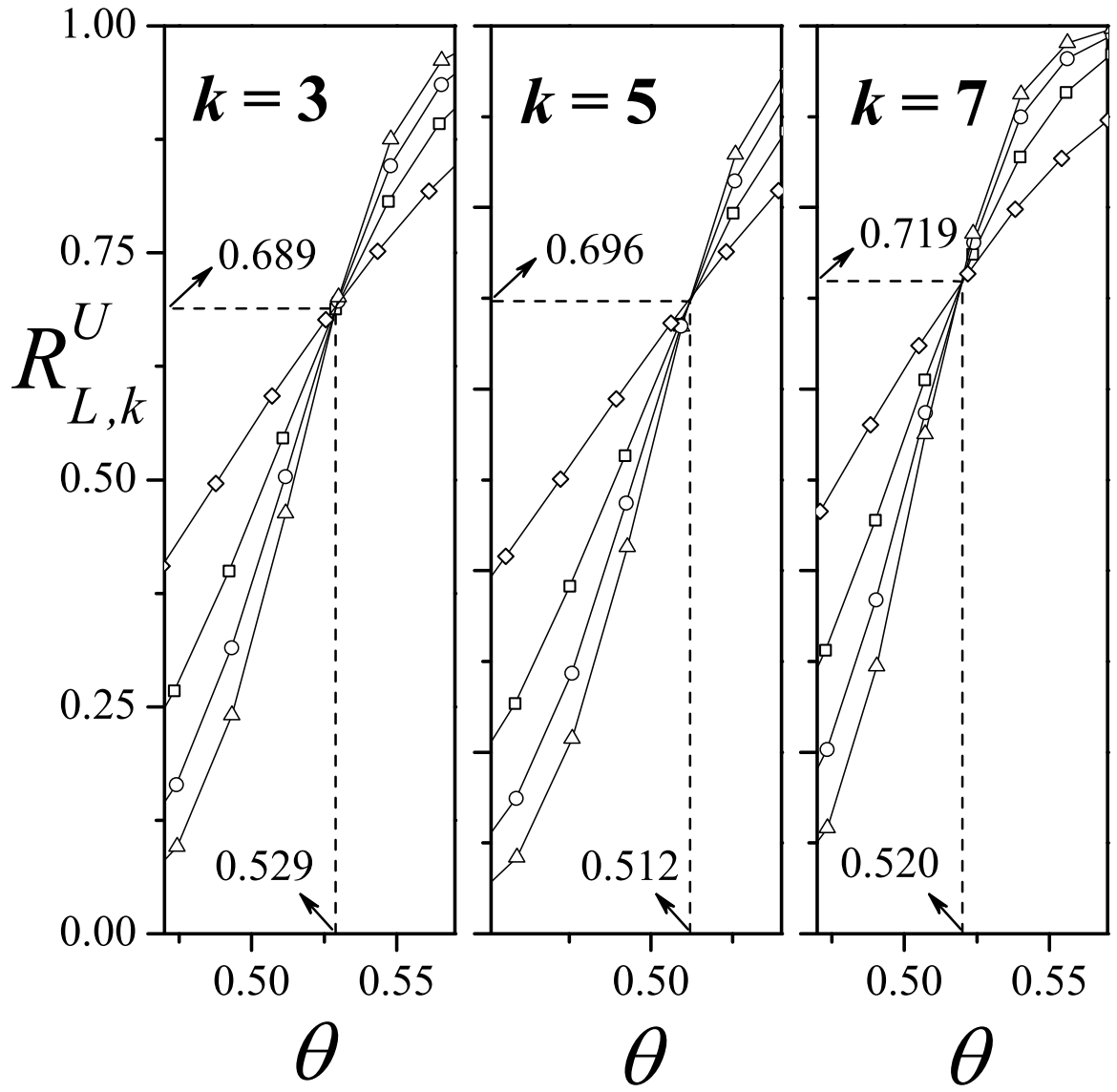


Fig. 1: D. A. Matoz-Fernandez et al.

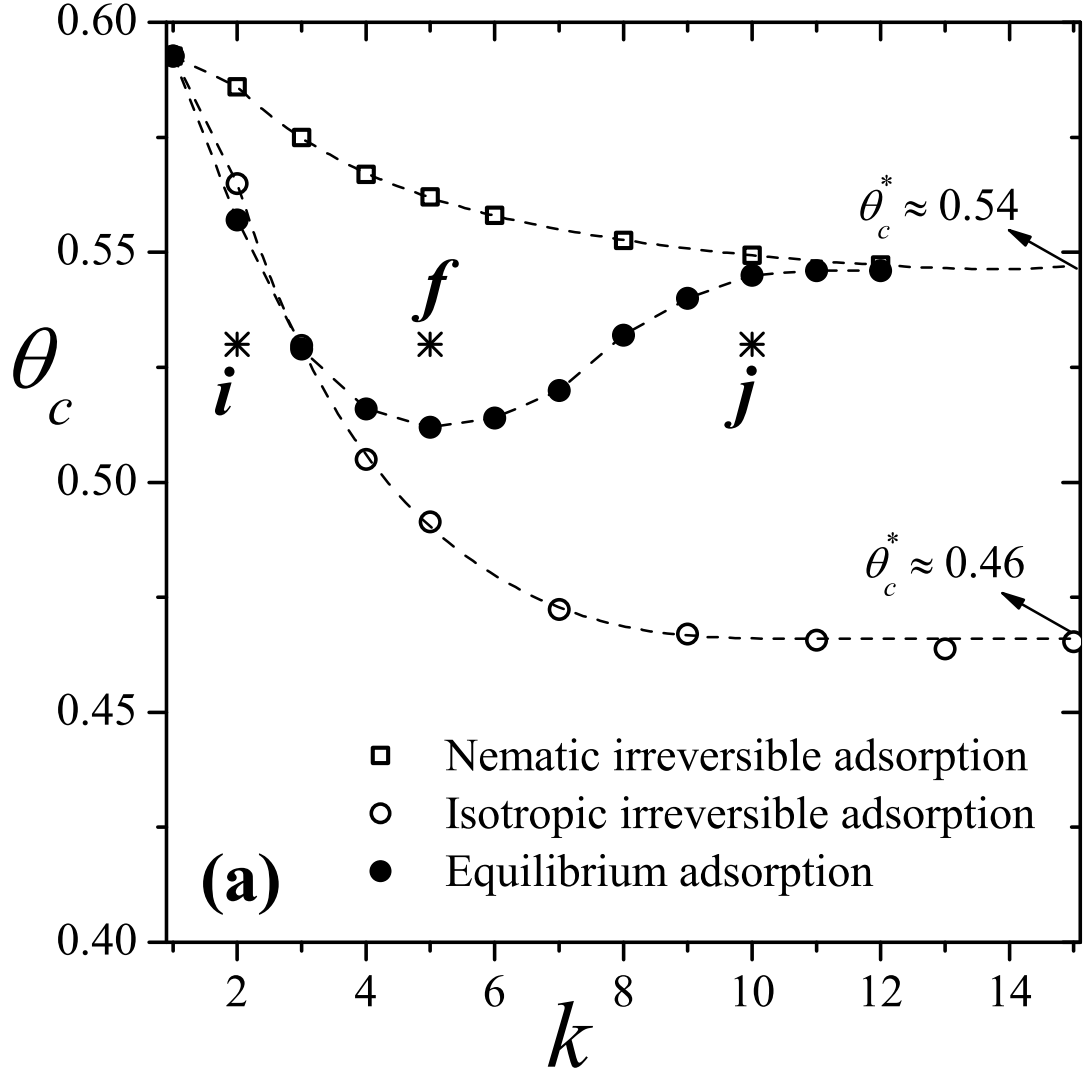
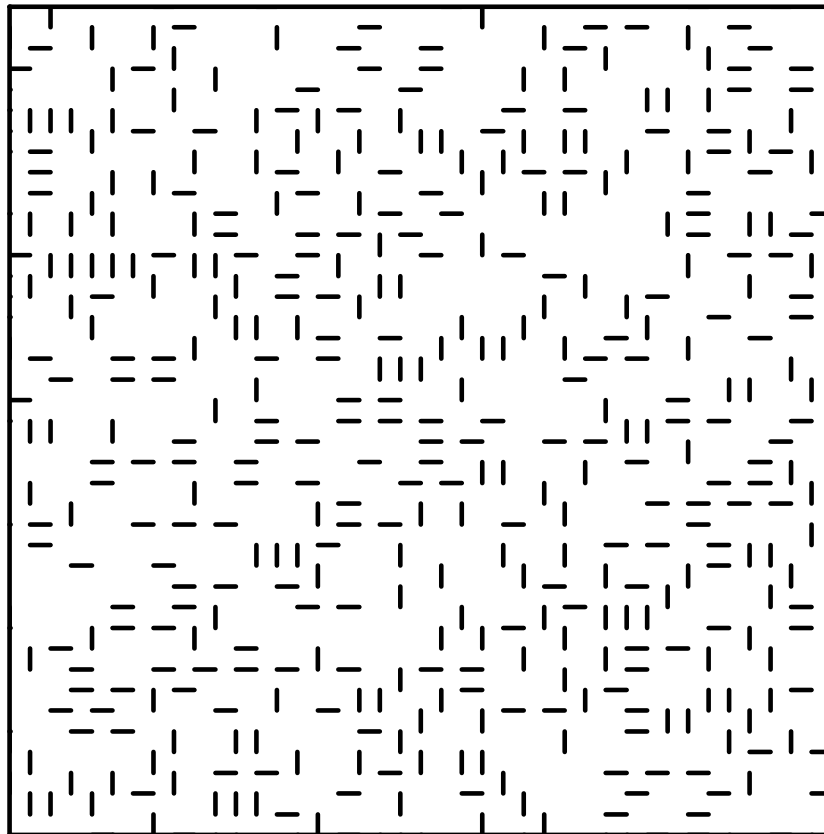


Fig. 2a: D. A. Matoz-Fernandez et al.



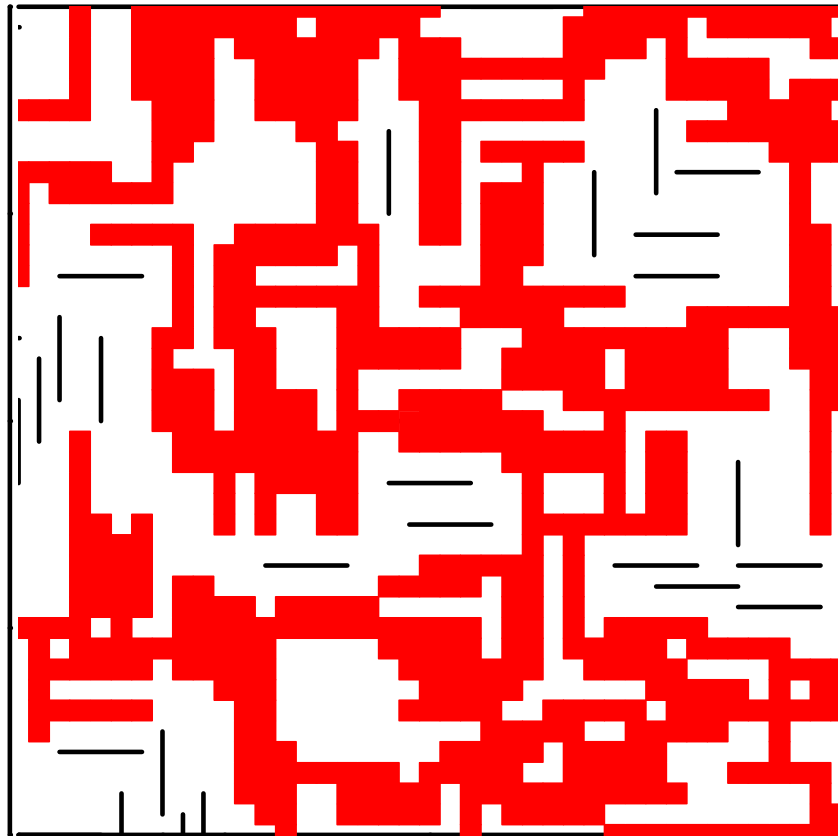
**Point  $i$ ,  $k = 2$**



**(b)**

Fig. 2b: D. A. Matoz-Fernandez et al.

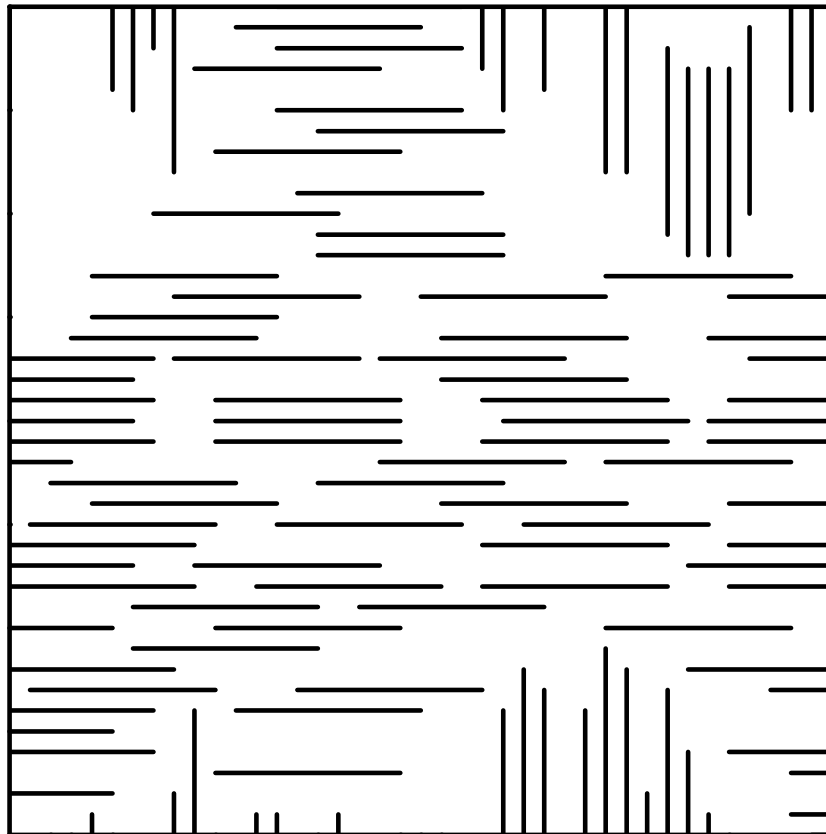
**Point  $f$ ,  $k = 5$**



**(c)**

Fig. 2c: D. A. Matoz-Fernandez et al.

**Point  $j, k = 10$**



**(d)**

Fig. 2d: D. A. Matoz-Fernandez et al.

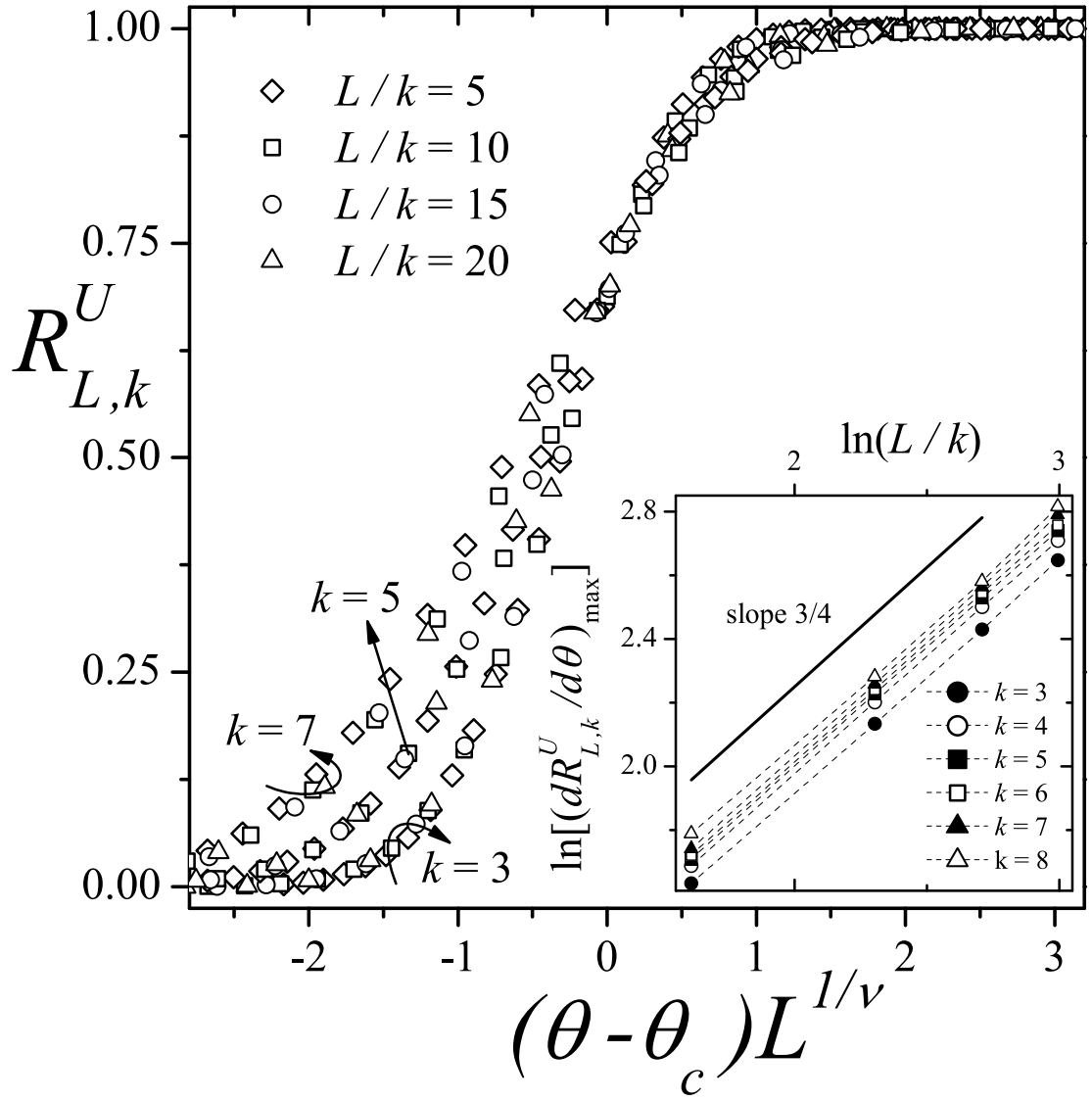


Fig. 3: D. A. Matoz-Fernandez et al.

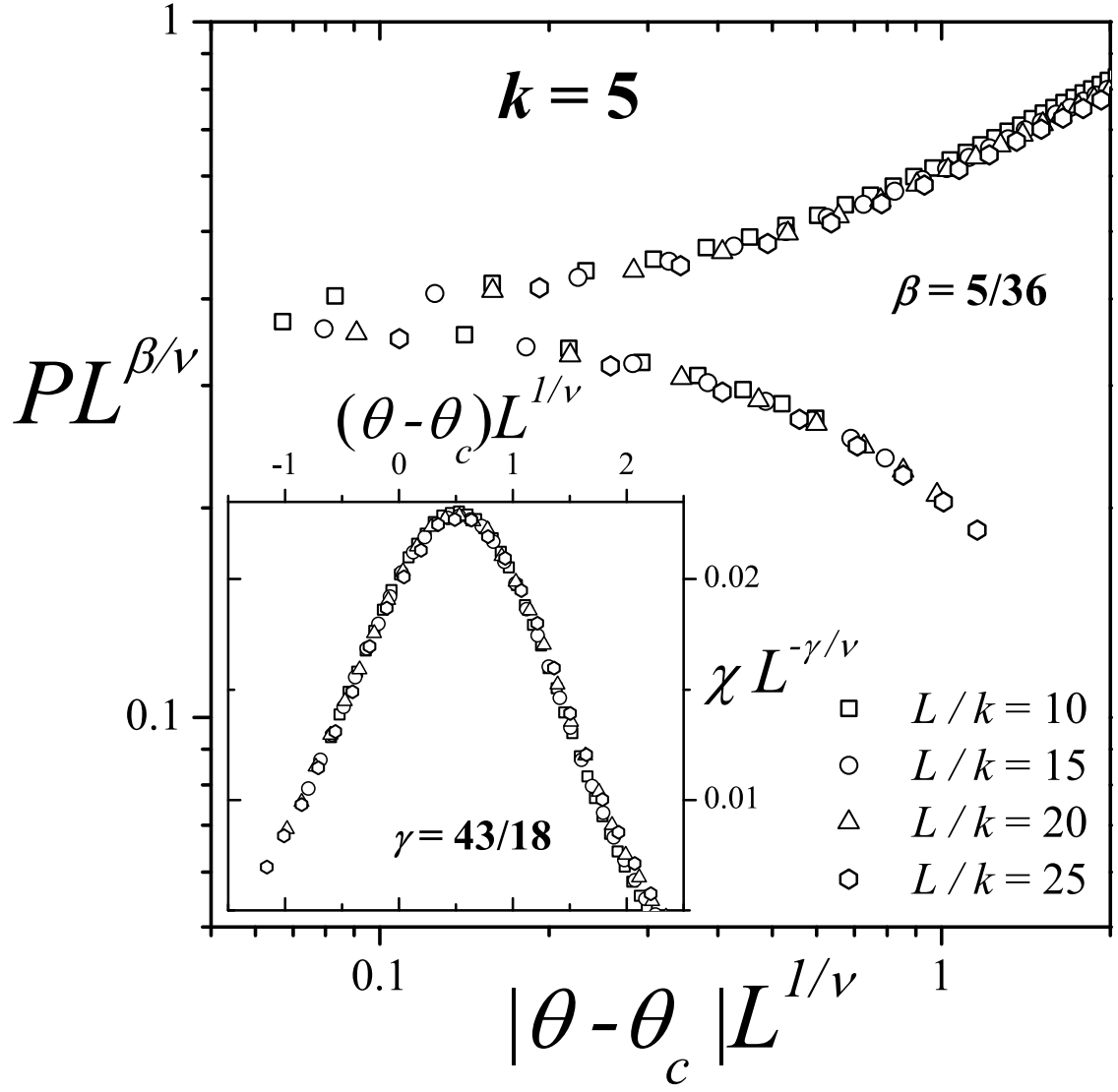


Fig. 4: D. A. Matoz-Fernandez et al.